Clays and Clay Minerals, Vol. 42, No. 1, 35–45, 1994.

CLAY MINERALS IN THE MACADAMS SANDSTONE, CALIFORNIA: IMPLICATIONS FOR SUBSTITUTION OF H_3O^+ AND H_2O AND METASTABILITY OF ILLITE*

WEI-TEH JIANG, DONALD R. PEACOR, AND ERIC J. ESSENE

Department of Geological Sciences, University of Michigan
Ann Arbor, Michigan 48109-1063

Abstract—Clay minerals from the MacAdams Sandstone, Kettleman North Dome, California, have been studied by electron microscopy. The clay minerals fill pore space associated with fractured and brecciated clasts of K-feldspar. Curved packets of muscovite and kaolinite are caused by deformation of detrital muscovite that resulted in opening of fissures subsequently filled with dominant kaolinite and minor intergrown mixed-layer illite/smectite (I/S). Regions of authigenic R1 I/S (rectorite) with characteristic ~20 Å periodicity are intergrown with kaolinite in microfissures within K-feldspar or detrital muscovite. Clusters of small grains of muscovite with nearly ideal composition occur as stacks and intergrown with kaolinite and are tentatively inferred to be authigenic. Contrary to previous reports, no illite was found in these samples.

Electron microprobe analyses previously obtained on Kettleman Dome "illite" and subsequently used as a prime example of analyses of illite rich in excess interlayer water (H_2O) and hydronium ion (H_3O^+) are shown to have been obtained on mixtures, and are not representative of the actual clay mineral compositions. Previous conclusions regarding significant H_3O^+ and H_2O contents of illite are invalid because of inaccuracies inherent in bulk and EMPA analyses of illite, and do not affect arguments regarding the metastability of illite. Hydronium substitution should be favored via the reaction $H_2O + H^+ = H_3O^+$ only in highly acidic fluids. Ordinary illite forming in sedimentary environments with carbonates and iron oxides is unlikely to have significant H_3O^+ substituted for K^+.

Key Words—Electron microscopy, Hydronium, Illite, Kaolinite, Muscovite, Rectorite.

INTRODUCTION

The question of whether clay minerals are in states of stable equilibrium in sedimentary and low-grade metamorphic rocks is critical to an understanding of the origins of those clay minerals. For example, the driving force for reactions involving clay minerals is determined by such relations, and such concepts are, therefore, basic to the genesis of clay minerals in prograde diagenetic and low-grade metamorphic sequences. The question regarding metastability is especially significant because clay minerals such as illite/smectite (I/S) are commonly used as indicators of temperature of formation, i.e., as geothermometers.

Geothermometers have largely been developed for applications to metamorphic rocks. Many geothermometers have eventually been found to be irrelevant 1) because they were not based firmly on states of stable equilibrium or 2) because all relevant variables in addition to temperature had not been constrained. After several decades of testing, a great number of reliable geothermometers have been developed (e.g., Essene, 1989). The validity of their application is now widely recognized to be based on experimental data for which equilibrium has been established; the determination that natural phases are in stable equilibrium; the constraint of all variables that affect the equilibrium state; and the accurate chemical and structural data on homogeneous phases. The question of the metastability of illite is, thus, a key factor in its use in determination of paleotemperatures.

Illite and its variants constitute some of the most abundant clay minerals, and illite is central to the widely studied reaction in which smectite is a reactant and illite (or mixed-layered I/S) is a product. Jiang *et al.* (1990a) reviewed the literature regarding metastability or stability of illite, emphasizing the ideas of Lippmann (1981, 1982). Lippmann concluded that illite is metastable, having a composition within the miscibility gap between muscovite and pyrophyllite. Jiang *et al.* provided direct transmission and analytical electron microscope (TEM and AEM) observations of pyrophyllite-muscovite pairs, corroborating Lippmann's hypothesis that only very limited solid solution occurs in muscovite equilibrated with pyrophyllite. Nonetheless, on the basis of available bulk illite analyses, Loucks (1991) concluded that white micas may have considerable H_2O and H_3O^+ contents that cause them to fall well outside of the binary pyrophyllite–muscovite system, hence rendering the arguments of Jiang *et al.* (1990a) inapplicable. Lippmann (personal communication, 1991) criticized Loucks' conclusion on several

* Contribution No. 496 from the Mineralogical Laboratory, Department of Geological Sciences.

grounds, emphasizing that high hydronium contents in common illite require unreasonably low pH values for the associated fluids.

Loucks (1991) relied in part on the electron microprobe analyses (EMPA) of Merino and Ransom (1982) for illite from Kettleman North Dome to infer the importance of H_3O^+ and H_2O substituted in illite. From the apparently low reported K^+ contents and low analytical totals, Loucks inferred high levels of H_3O^+ and H_2O substituted in Kettleman illite. This inference ignores the effects of poor sample polish, the analysis of multiphase materials, and the likelihood of substantial specimen damage during the EMPA of small particles. Loucks constructed phase diagrams for the stability of illite and muscovite solid solutions on the joins $KAl_2Si_3AlO_{10}(OH)_2$–$(H_2O)Al_2Si_4O_{10}(OH)_2$ ("pyrophyllite hydrate") and $KAl_2Si_3AlO_{10}(OH)_2$–$(H_3O)Al_2Si_3AlO_{10}(OH)_2$ ("hydronium muscovite") from his interpretations of published analytical data. He concluded that illite has extensive stable substitution of hydronium muscovite and pyrophyllite hydrate, rather than being approximated as an intermediate solid solution of pyrophyllite and muscovite.

Analytical electron microscope analyses of clay minerals in soils, sedimentary rocks, and low-grade metamorphic rocks reveal that several clay minerals are commonly intergrown (e.g., Peacor, 1992). Clay minerals that appear to be homogeneous at the level of optical or scanning electron microscope (SEM) observations, therefore, often yield EMPA and bulk analyses that correspond to mixtures. Inferences of K^+ deficiencies and of H_3O^+ and H_2O contents from EMPA or bulk analyses of illites that contain interlayers of smectite, chlorite, or kaolinite may, therefore, be flawed. Even though great care may be utilized to obtain the finest fractions in mineral separates that have been commonly assumed out of necessity to include only a single clay mineral, TEM observations invariably show significant amounts of contaminating phases and heterogeneity (e.g., Ohr *et al.,* 1991). Wet chemical analyses of clay minerals are, therefore, invariably subject to contamination (Warren and Ransom, 1992).

Loucks (1991) selected chemical analyses of illite that satisfied stringent criteria. We have carried out a TEM-AEM study of clay minerals from drill cores of the Eocene MacAdams Sandstone, Kettleman North Dome, California, because the EMPA analyses of Merino and Ransom (1982) served as Loucks' key illustration of conclusions regarding H_2O and H_3O^+ contents of white micas. Merino kindly donated the original thin sections from which the EMPA analyses of Merino and Ransom (1982) had been obtained. The Kettleman Dome structure is located in the Kettleman Hills south of Coalinga on the west side of the Great Valley of California. It formed by mid-Pleistocene deformation of the thick Cretaceous and Tertiary sedimentary pile in the Great Valley (Merino, 1975a, and references therein) and was a target for oil and gas exploration in central California (Norris and Webb, 1990). Merino (1975a) described the diagenetic mineral relations, including the clay diagenesis that occurred in the MacAdams Sandstone, perhaps soon after deposition in the Eocene and during Pleistocene deformation. The relations between authigenic minerals and pore fluids were analyzed in Merino (1975b).

We have obtained AEM analyses of clay minerals from the MacAdams Sandstone shown by TEM to consist of single phases. The AEM and TEM data show that the original EMPA analyses corresponded to clay mixtures, implying that Loucks' conclusions are invalid. The data are presented in order to illustrate some relations among clay minerals in a diagenetic regime, to test the possibility of hydronium substitution in illite as postulated by Loucks on the basis of analyses of the same samples, and to evaluate the possibility that such data obviate the conclusion of Jiang *et al.* (1990a) that illite is a metastable phase.

ANALYTICAL TECHNIQUES

Thin sections were first studied by optical microscopy and SEM using a Hitachi S-570 SEM fitted with a back-scattered electron (BSE) detector and Kevex Quantum energy-dispersive analytical (EDA) system to define large-scale textural relations and locate the so-called illite, which could then be studied by TEM/AEM. The sections were attached with epoxy and could not be easily removed, so TEM samples were prepared by attaching the polished sample surface to a glass slide with "sticky wax," grinding away the original glass slide and epoxy, attaching a 3-mm-diameter Al washer to the newly polished surface with epoxy, and then removing the 3-mm-diameter area of interest from the sticky-wax backed slide with gentle heating. The samples were then ion milled in order to obtain electron-transparent thin edges. Such samples were first examined using the SEM to locate regions of ion-milled thin edges of interest and then studied by TEM with a Philips CM-12 scanning transmission electron microscope (STEM) fitted with a Kevex Quantum EDA system. Chemical analyses were obtained only for areas that were shown to consist of structurally homogeneous minerals by TEM (including lattice-fringe images) and selected-area electron diffraction (SAED). All analyses were obtained in STEM mode with the beam rastered over areas as large as 2000 Å square in order to minimize alkali diffusion. Analyses of unknowns were obtained under conditions used for determination of standard k-values in order to minimize error due to alkali diffusion (van der Pluijm *et al.,* 1988). The EDA data were processed using Kevex software, and resulting intensity ratios were converted to concentration ratios using k-values obtained with muscovite (Al, K); phengitic muscovite (Mg, Al, K, Fe); K-feldspar (Al, K); albite (Na, Al); chlorite (Mg, Al, Fe); jadeite (Na, Al);

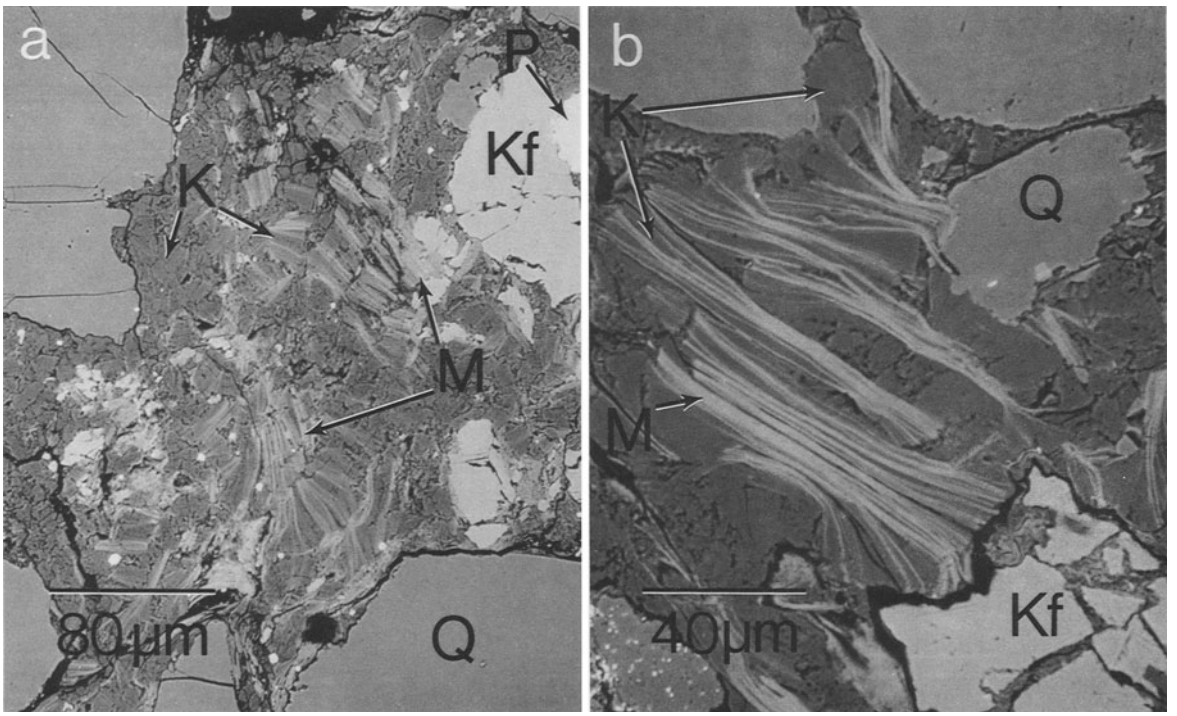

Figure 1. a) Back-scattered electron image of deformed detrital muscovite (M) with kaolinite (K) filling interlayer fissures, and separate detrital muscovite, authigenic kaolinite, pyrite (P), and angular K-feldspar (Kf) in pore space between quartz (Q) grains with serrated surfaces indicating dissolution. b) Higher-resolution image showing features similar to those of (a), but with greater detail in the detrital muscovite-kaolinite intergrowths (some of the kaolinite is actually a mixture of kaolinite and I/S). Brecciated feldspar has a rounded, serrated surface implying dissolution.

fayalite (Fe); paragonite (Na, Al); phlogopite (Mg, Al, K); wollastonite (Ca); rhodonite (Ca, Mn, Fe); biotite (Mg, Al, K, Ti, Fe); and sphene (Ca, Ti) as standards (elements for which k-values were determined in parentheses).

RESULTS

Figure 1a is a low-magnification BSE image of a Kettleman North Dome sample that illustrates textures typical of the clay mineral occurrences. The sample is dominated by grains of detrital quartz with clay minerals occupying pore space. The quartz grains have abundant cracks and serrated, rounded surfaces that imply that they have undergone dissolution. Angular, cracked, and often brecciated K-feldspar grains commonly occupy much of the space between quartz grains, but the surface of the feldspar grains is locally rounded and serrated. The feldspar is homogeneous, nearly end-member K-feldspar (Or_{96}, Table 1), as indicated by homogeneity in BSE images, EDA analyses using the SEM, and EMPA analyses. Partial albitization was observed in one of the K-feldspar grains. The modified

Table 1. Representative analytical electron microscope analyses of detrital muscovite, K-feldspar, and mixtures of kaolinite + detrital muscovite in sample 890-E72-9933 of the McAdams Sandstone.[1]

	Si	Al	Mg	Fe^{3+}	Ti	Mn	K	Na	Ca
Musc	6.09	5.46	0.14	0.26	0.05	0	1.96	0.07	0
Musc	6.14	5.42	0.14	0.23	0.06	0	1.90	0.06	0
Musc	6.14	5.35	0.14	0.28	0.09	0	1.92	0	0
Musc	6.06	5.47	0.14	0.27	0.06	0	1.90	0.06	0
Musc	6.13	5.41	0.14	0.24	0.09	0	1.89	0.10	0
Mix	6.16	5.65	0.09	0.10	0	0	0.62	0	0
Mix	6.18	5.54	0.10	0.14	0.04	0	0.92	0	0
K-feld	2.96	1.02	0	0.01	0.01	0	0.91	0.04	0

[1] Normalization is based on 12 tetrahedral and octahedral cations total for muscovite; mixtures of muscovite + kaolinite; and 4 for K-feldspar.

https://doi.org/10.1346/CCMN.1994.0420105 Published online by Cambridge University Press

Table 2. Representative analytical electron microscope analyses of authigenic muscovite, mixed-layer illite/smectite, and kaolinite in sample 890-E72-9933 of the McAdams Sandstone.[1]

	Si	Al	Mg	Fe^{tot}	Ti	Mn	K	Na	Ca
Musc	5.94	5.25	0	0.57	0.14	0	2.02	0	0
Musc	5.95	5.42	0	0.55	0.08	0	2.00	0	0
Musc	6.06	5.33	0.04	0.50	0.07	0	2.06	0	0
Musc	6.02	5.48	0	0.50	0	0	2.02	0	0
I/S	6.42	5.44	0.07	0.07	0	0	1.35	0	0
I/S	6.58	5.35	0.08	0.09	0	0	1.33	0.07	0
I/S	6.51	5.36	0.07	0.06	0	0	1.28	0.05	0
Kaol	7.97	7.97	0	0.06	0	0	0	0	0

[1] Normalization is based on 12 tetrahedral and octahedral cations total for muscovite and mixed-layer illite/smectite, and 16 for kaolinite.

angular shapes are consistent with deformation and dissolution of detrital grains, but the end-member composition implies equilibration with a pore fluid during diagenesis.

The clay minerals occupy the pore space between quartz grains and are closely associated with K-feldspar. Figure 1a illustrates curved, lath-like grains with bright contrast consisting of muscovite separated by lenticular kaolinite having dark contrast. Kaolinite also commonly occurs as separate grains coexisting with chlorite, muscovite, or I/S; it is chemically homogeneous (Table 2), regardless of the identity of the coexisting phases. Figure 1b shows muscovite–kaolinite stacks at higher magnification. The muscovite consists of curved, deformed packets of parallel 001 layers separated by kaolinite. Stacks of clay minerals with similar textures have been described by many workers (e.g., Pye and Krinsley, 1983; Primmer and Shaw, 1987; Morad, 1990) and have been inferred to have been caused by deformation of detrital grains with production of fissures and subsequent infilling by an authigenic phase (e.g., van der Pluijm and Kaars-Sijpesteijn, 1984; Li *et al.*, 1993). Stress is inferred in this case to have caused separation of muscovite layers with subsequent crystallization of kaolinite in the resulting fissures and the associated pore space.

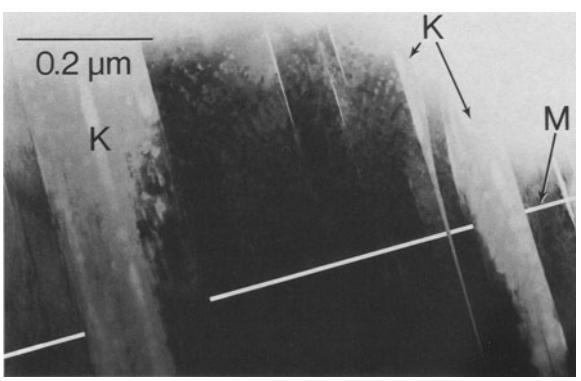

Figure 2. Low-resolution TEM image showing interlamination of kaolinite (K) and detrital muscovite (M).

Table 1 shows that the detrital muscovite has a composition corresponding to a mature mica: The number of $^{[VI]}Al$ is near four, and the number of interlayer cations, largely K, is near two. Such a composition is typical of mature muscovite (i.e., well-ordered polytype, usually $2M_1$; near end-member composition, $^{[IV]}Al/Si = 1/3$; relatively large grain size) from a relatively high-temperature igneous or metamorphic environment, in contrast with typical illite or I/S (disordered stacking sequence; K- and Al-deficient; grains a few tens of layers in thickness) that forms in low-temperature environments (Peacor, 1992). Figure 2 is a low-resolution TEM image showing zones that consist of kaolinite aligned parallel or subparallel to (001) of packets of detrital muscovite. Figure 3a shows a

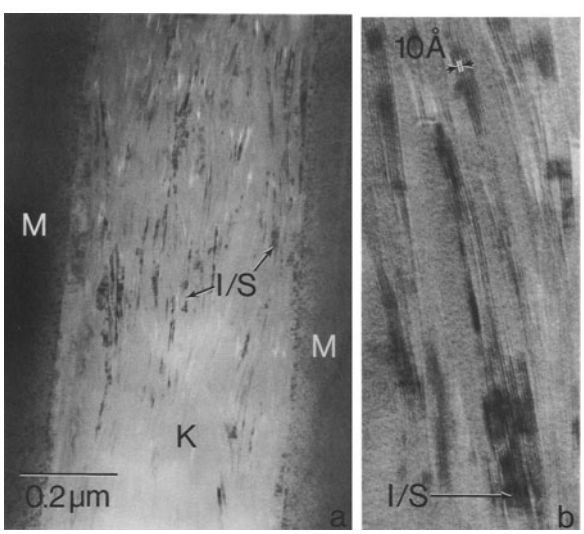

Figure 3. a) TEM image showing a mixture of curved, discontinuous packets of kaolinite (K) and mixed-layer illite/smectite (I/S) (mottled appearance) filling a fissure in detrital muscovite. The boundary of the muscovite is largely defined by a single, continuous layer. b) Lattice-fringe image of packets of mixed-layer illite/smectite (showing mottled texture and fringes) surrounded by kaolinite that occupies most of the area without fringes. The area shown is a part of that shown in (b).

https://doi.org/10.1346/CCMN.1994.0420105 Published online by Cambridge University Press

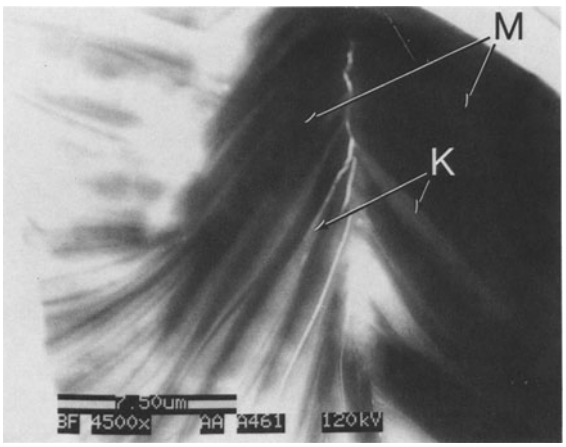

Figure 4. Scanning transmission electron image of folded detrital muscovite (M) interleaved with kaolinite (K). The kaolinite layers are randomly distributed in two limbs of the microfold, implying fissure filling after deformation.

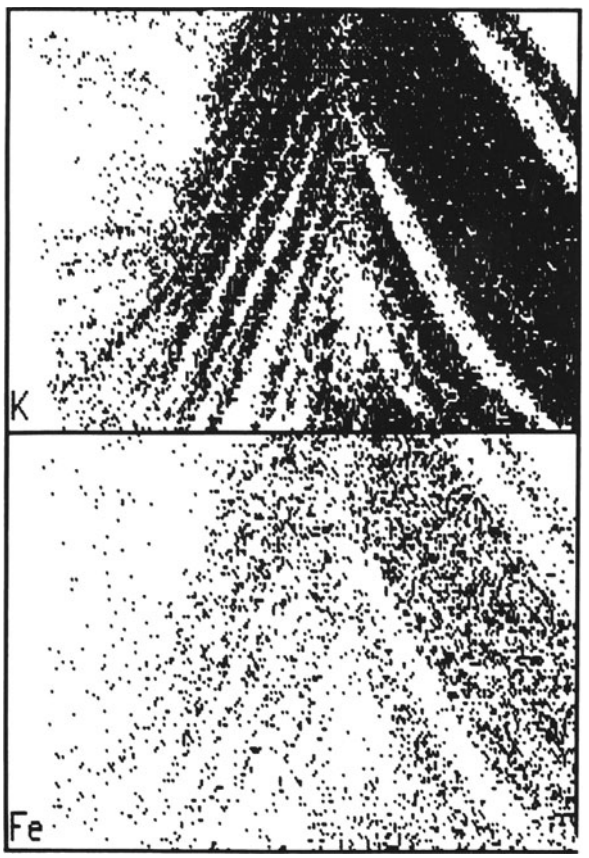

Figure 5. Element X-ray maps of folded detrital muscovite interlaminated with kaolinite. The distribution of Fe matches that of K+ and corresponds to the muscovite. The mapped area is approximately the same as the imaged area in Figure 4.

mixture of dominant kaolinite and packets of a material identified as ordered mixed-layered I/S (verified by SAED, lattice fringe images, and AEM analyses), filling a fissure within detrital muscovite. The I/S displays the mottled appearance typical of many 2:1 minerals as a result of electron-beam damage. The muscovite has straight, uninterrupted layers parallel to the interface, whereas the complex I/S-kaolinite mixture consists of subparallel, discontinuous packets of layers consistent with the interpretation that kaolinite and I/S filled stress-caused fissures in detrital muscovite that originally consisted of a crystal with contiguous, parallel, coherent layers.

Figure 3b is a HRTEM lattice fringe image showing thin packets of I/S layers having mottled contrast and lattice spacings of around 10 Å. Areas of the figure that have no lattice fringes consist largely of kaolinite. Kaolinite is subject to very rapid beam damage, and the lattice fringes of kaolinite usually deteriorate before a photograph can be obtained. The identification was verified by AEM (Table 1) and SAED patterns obtained before damage was incurred. Formation of kaolinite in fissures in muscovite without formation of I/S was also observed. Figure 4 shows a transmitted electron image of a grain of detrital muscovite having fissures filled with kaolinite that was obtained in STEM mode. The muscovite grain is folded and the kaolinite layers are discontinuous and unrelated on two limbs, implying that the kaolinite formed after the deformation of the muscovite. Figure 5 shows element maps of the folded grain in Figure 4. The higher Fe content of the muscovite correlates directly with its K^+ content, consistent with direct AEM analyses.

Figure 6 illustrates a second kind of mica occurring with kaolinite. This muscovite also occurs as stacks intergrown with kaolinite, but differs in several ways from the detrital muscovite described above. AEM analyses (Table 2) show that it has almost no Mg, higher Fe^{3+}, and virtually no detectable Na. It occurs in aggregates of approximately equal-diameter, small grains. No deformation features are observed. The mature, mica-like formula and kaolinite intergrowths are consistent with a detrital origin; but the small crystal size, occurrence as equidimensional aggregates, and lack of deformation features, especially as contrasted with the mica of clear detrital origin, imply an authigenic origin. We tentatively infer that this mica crystallized from pore fluids at some unspecified stage in the development of the pore-filling minerals, probably preceding formation of kaolinite. Although the conclusion regarding the origin of this mica is problematic, it has no bearing on the conclusions discussed below.

Figure 7a is a low-resolution SEM/BSE image showing a clay mineral defined as I/S and occurring as packets of irregular shape within brecciated K-feldspar. Packets of I/S appear to be separated by irregular areas of dark contrast. In some cases those areas are unoccupied; such spaces commonly result from dehydration

https://doi.org/10.1346/CCMN.1994.0420105 Published online by Cambridge University Press

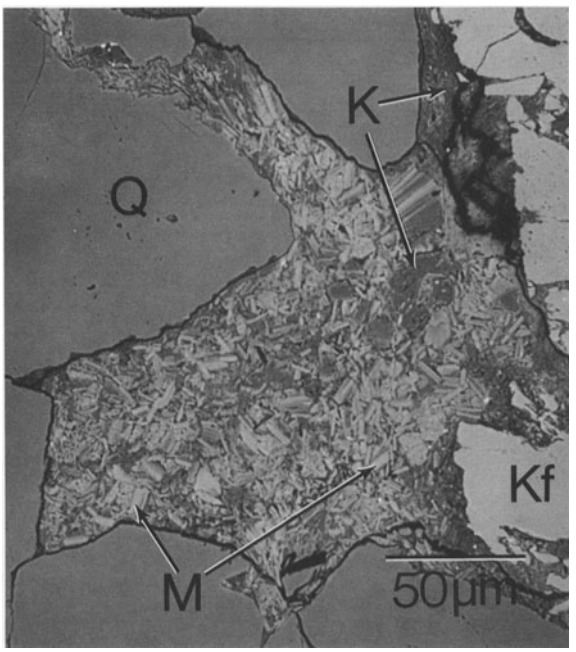

Figure 6. Back-scattered electron image showing crystals of authigenic(?) muscovite (M) associated with kaolinite (K) and brecciated K-feldspar (Kf) in pore space within quartz (Q).

of the smectite interlayers of I/S in the vacuum of the ion mill or STEM, giving rise to contraction in $d(001)$ of around 14–10 Å. However, some of the areas of dark contrast consist of kaolinite. Figure 7b is a higher resolution SEM/BSE image showing that rounded areas consisting largely of kaolinite are intergrown with the I/S. The feldspar displays rounded serrated edges typical of dissolution, implying a lack of equilibrium between fluids and K-feldspar at the time of origin of those features. Assuming that authigenic clay minerals crystallized from pore fluids concomitant with feldspar dissolution, such a relation implies lack of equilibrium between K-feldspar and the clay minerals. The pore-filling textures of the randomly oriented, very small clay flakes suggest an origin of direct precipitation from fluids. The I/S invariably occurs filling pore space or in fissures in detrital muscovite.

Figure 8 is a low-resolution TEM image showing typical I/S packets separated by shrinkage cracks and in direct association with K-feldspar. Figure 9a is an HRTEM lattice fringe image of I/S taken under overfocus conditions. It shows alternating dark and light fringes corresponding to smectite and illite layers (e.g., Veblen *et al.*, 1990; Jiang *et al.*, 1990b), individual fringes separated by ~10 Å illite-like and 10–12 Å dehydrated smectite-like layers. The dark fringes have ~20 Å periodicity characteristic of dehydrated rectorite or R1 I/S, although some three-layer repeat units can be seen. Figure 9b shows a packet that consists largely of R2 I/S having periodicity of 30 Å. The diffraction pattern (Figure 9c) corresponding to the lattice fringe image of Figure 9a displays a prominent 20 Å sequence of reflections, with diffuse non-00*l* reflections indicating a high degree of stacking disorder (Peacor, 1992) consistent with dominant $1M_d$ polytypism. The presence of discrete, albeit extremely diffuse, non-00*l* reflections is consistent with some local stacking order.

As shown by the AEM analyses, the I/S has a composition very different from that of the micas (Table 2). The $^{[VI]}$Al contents are approximately 1.5 and interlayer cations total approximately 1.35. The normalized formulae have a slight excess of negative charge, probably corresponding to some K^+ loss during analysis (van der Pluijm *et al.*, 1988), but the imbalance is small. The Kettleman North Dome I/S, or rectorite, has a composition similar to that of authigenic illite in general (e.g., Lanson and Champion, 1991; Jahren and Aagaard, 1992; Ireland *et al.*, 1983; Macchi *et al.*, 1990; Burley, 1984); there are around 1.5 $^{[IV]}$Al and 1.4 interlayer cations per 12 [IV] + [VI], and the net negative charge is approximately 0.7–0.8 per half unit cell (Table 2). Such a composition does not correspond to an average of illite-like and smectite-like layers, and it must be related to unique aspects of the ordered rectorite structure via simple ordering of smectite and illite layers (Ahn and Peacor, 1986; Jiang *et al.*, 1990b). Such relations indicate that the composition range of ordered rectorite or R1 I/S corresponds approximately to that normally associated with illite. Those minerals, therefore, cannot be differentiated solely on the basis of chemical composition (Jiang *et al.*, 1992).

DISCUSSION

Formation of mica-kaolinite intergrowths

The mica component of the interlaminated muscovite-kaolinite-I/S grains has a composition that is typical of mature muscovite occurring in metamorphic rocks in that there is some octahedral Fe and Mg, the interlayer cation contents are near two, and the $^{[IV]}$Si content is only slightly greater than six (per 12 [IV] + [VI]). The curved layers, fractured quartz, and brecciated feldspar imply that detrital minerals have been subjected to considerable stress. Many authors have described similar clay mineral stacks (e.g., Pye and Krinsley, 1983; Primmer and Shaw, 1987; Morad, 1990), and Li *et al.* (1993) reviewed the evidence for separation of layers, production of elongated fissures, and precipitation of another phyllosilicate within fissures so as to produce interlaminated phyllosilicates of two different ages. Although the muscovite of this study occurs in packets of constant thickness along layers for which the boundaries consist largely of single layers, kaolinite units often have a lenticular shape. High-resolution images show that kaolinite occurs as subparallel packets intergrown with packets of I/S. Layers are discontinuous, commonly subparallel or nonparallel, and terminate against continuous bonding

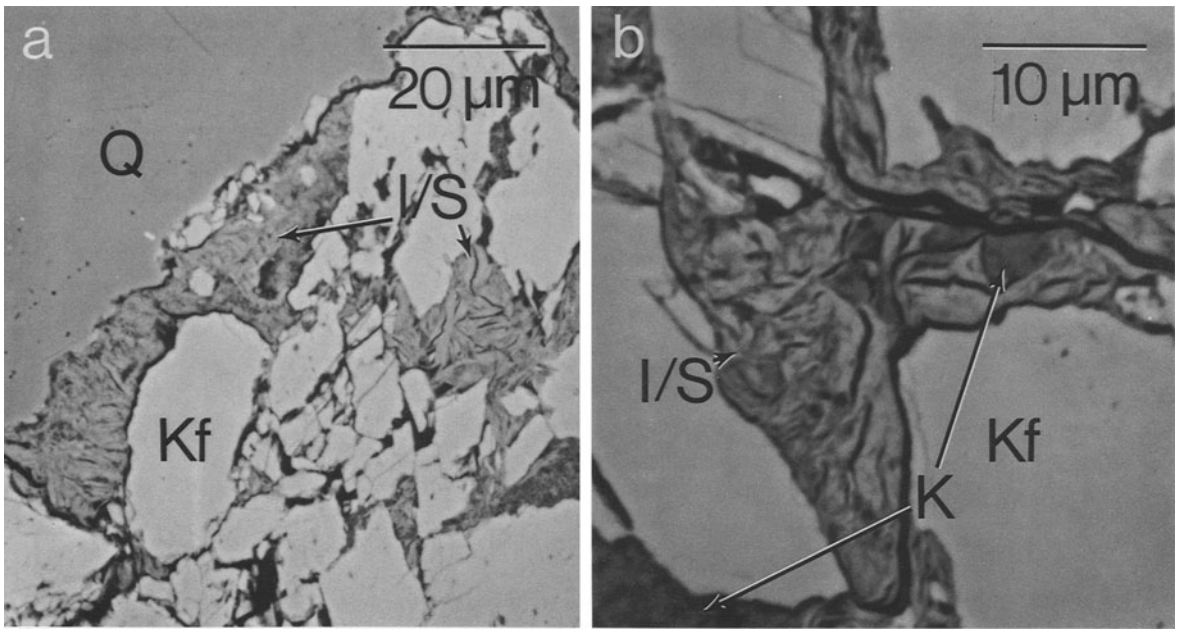

Figure 7. a) Back-scattered electron image showing rectorite (R1) mixed-layer illite/smectite (I/S) and kaolinite (K) embayed between quartz and brecciated K-feldspar (Kf). b) Higher-magnification image (2000×) of rectorite filling space between clasts of brecciated K-feldspar. The dark areas within rectorite consist largely of kaolinite. The elongated fissures are, in part, caused by shrinkage of mixed-layer illite/smectite but locally consist of kaolinite.

muscovite layers. Such textures are consistent with deformation of already-formed mica and with subsequent precipitation of kaolinite and I/S.

The observations of textural relations of this study permit some speculation concerning the nature of the equilibrium assemblages. First, the surfaces of quartz and K-feldspar clearly show the effects of some dissolution, therefore implying disequilibrium with the pore-filling phases if dissolution occurred at the same time as precipitation of phyllosilicates. The I/S and kaolinite show textures clearly demonstrating that they formed together; however, the textural relations with the muscovite tentatively inferred to be authigenic are not clearly defined. The occurrence of small flakes of I/S in microfissures intimately associated with detrital muscovite or K-feldspar implies that the I/S formed metastably in areas where the chemical gradient involving K^+ was large. The ragged nature of the quartz and K-feldspar grains suggests that the diagenetic solutions were undersaturated in SiO_2 and $KAlSi_3O_8$. The muscovite that was tentatively inferred to be authigenic may have formed by progress of the irreversible reaction, K-feldspar + kaolinite = muscovite + SiO_2 (aq) + H_2O.

Compositions of clay minerals

Collectively the TEM/AEM results show that clay minerals occur as intergrowths at a scale smaller than that resolvable by optical or SEM techniques, implying that it is not possible to obtain EMPA analyses of single clay minerals (Peacor, 1992). Even in the case of detrital muscovite-kaolinite intergrowths studied here, which were partially resolved by optical and SEM imaging, finer intergrowths were observed at higher TEM resolution. In order to make a practical test of the ability of EMPA to resolve the compositions of individual phases as implied by Merino and Ransom (1982),

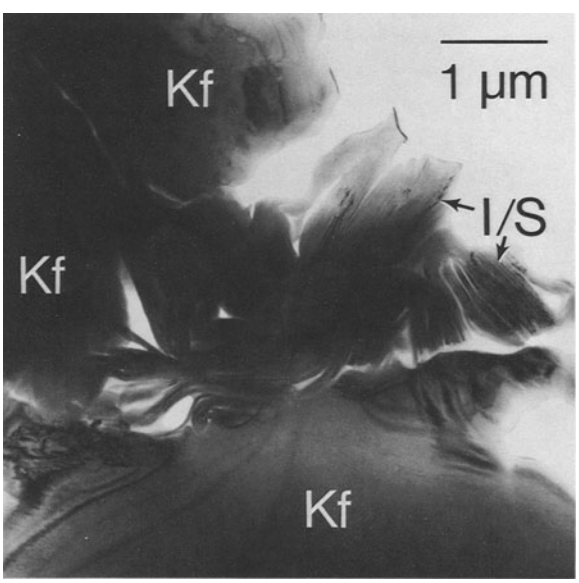

Figure 8. Low-resolution TEM image of mixed-layer illite/smectite (I/S) associated with K-feldspar (Kf).

https://doi.org/10.1346/CCMN.1994.0420105 Published online by Cambridge University Press

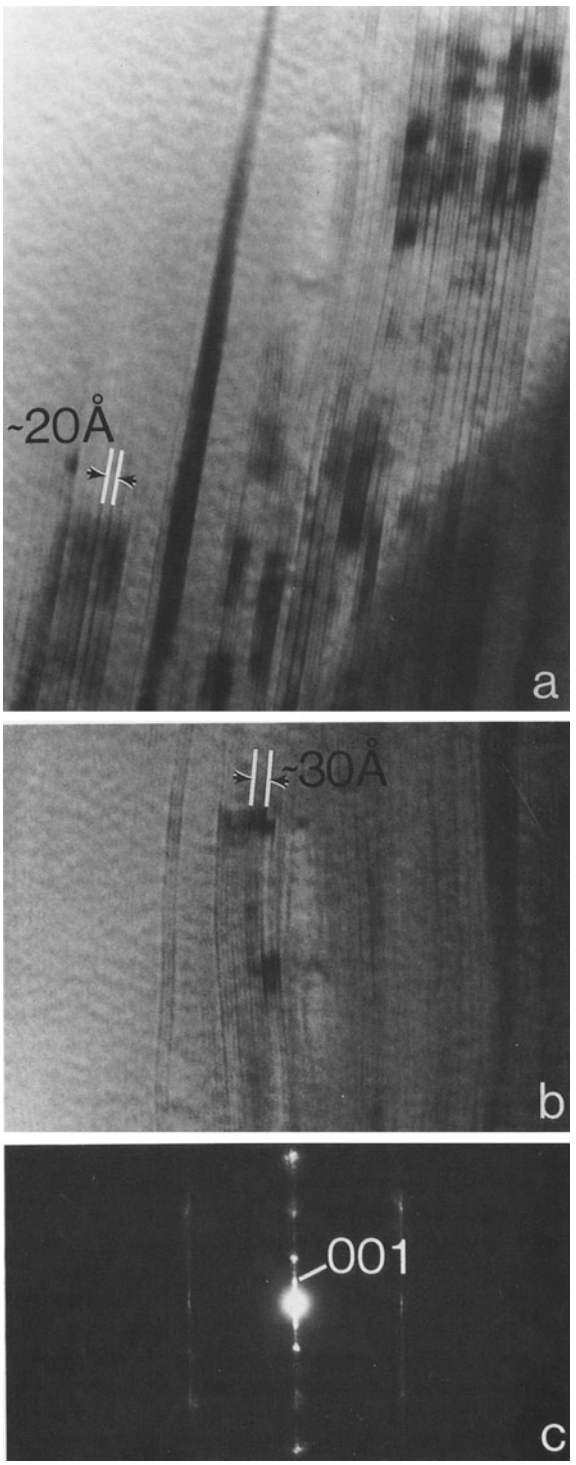

Figure 9. Lattice-fringe images and selected-area electron diffraction pattern of mixed-layer illite/smectite. The alternating dark and light fringes correspond to smectite-like and illite-like interlayers, respectively. a) Dark layers define an area composed largely of R1 mixed-layer illite/smectite (rectorite) having ~20 Å periodicity. b) Thin packet of R2 mixed-layer illite/smectite having ~30 Å periodicity. c) electron diffraction pattern of rectorite in (a) showing ~20 Å periodicity in 001 reflections. Non-001 reflections are Okl. They are markedly diffuse, indicating polytypic stacking disorder, but the lack of h0l reflections indicates a lack of turbostratic stacking.

we made an attempt to obtain EMPA analyses utilizing optical imaging, but the lack of significant contrast and smooth polishing surfaces between clay minerals resulted in severe beam overlap in all cases. Even when BSE was used for imaging, EMPA analyses were of mixtures, as expected on the basis of TEM observations. Although based on the most careful optical study possible at the time, the EMPA analyses obtained by Merino and Ransom (1982) must, therefore, have corresponded to mixtures. Their analyses were obtained with a larger than usual beam in order to minimize alkali diffusion and without the benefit of BSE imaging. They show significant deficiencies in alkali atoms and low analytical totals relative to values expected for illite, even though great care was used to minimize diffusion of alkalis. Such apparent deficiencies are the natural result of obtaining data on mixtures of I/S and/or muscovite with kaolinite.

The muscovite-kaolinite-I/S mixtures were originally identified as illite, a natural conclusion that was based in part on optical and EMPA data. As we have not been able to observe illite in the same specimens that were characterized by Merino and Ransom as containing illite, it is not possible to arrive at conclusions regarding illite on the basis of these samples. Our AEM data on the same samples reveal detrital muscovite, authigenic(?) muscovite of nearly ideal composition, and I/S with normal interlayer cation contents but certainly no illite nor other 10 Å phyllosilicates with very low K^+ contents. The six chemical analyses of so-called alkali-poor illite from Kettleman Hills, which were used by Loucks (1991) as outstanding examples of extensive H_2O and H_3O^+ substitutions in natural illite, are, therefore, erroneous. Loucks concluded, "These natural illite compositions are remarkably close to the join $(H_2O)Al_2Si_4O_{10}(OH)_2$–$(H_3O)Al_2Si_3AlO_{10}(OH)_2$." These analyses were not included with his superior data set because there were no analyses for water, but they contributed significantly to the locus of his inferred phase boundaries for illite solid solutions. Loucks argued that Merino and Ransom's use of a very low beam current yielded very small excitation volumes during analysis of their illites. This is an erroneous interpretation: Only diminishment of operating voltage can decrease excitation volumes during electron microbeam analyses of thick specimens (Reed, 1975). Beam damage—yielding apparently low alkali site occupancies, low analytical totals, and, therefore, high inferred H_2O contents—

https://doi.org/10.1346/CCMN.1994.0420105 Published online by Cambridge University Press

must be anticipated during electron microbeam analysis of any fine-grained mica, illite, and smectite.

Our TEM observations of illite, I/S, and other clay minerals of soils, sedimentary rocks, and low-grade metamorphic rocks reveal that they are ubiquitously intergrown as heterogeneous materials at a scale of a few thousand Ångstroms or less, at scales that cannot be resolved optically by EMPA or by SEM (Peacor, 1992). Therefore, EMPA analyses of such materials, especially illite, can rarely, if ever, be obtained from pure single-phase clay minerals. Such analyses must always be cautiously utilized, as some contamination must almost invariably be present. Because all phyllosilicates have certain chemical features in common, contaminants may not appear to produce obvious errors, except for high H_2O and low K^+ contents, and indeed may be misinterpreted as depicting interesting solid solution variants. A prime example is in the analyses of Merino and Ransom that were utilized by Loucks.

The same problems are even more vexing with respect to wet chemical analyses of bulk clay mineral separates. Even utilizing the carefully separated <0.1 μm fraction of shales (measured as such by TEM), we find significant amounts of several minerals, each one of which may not be detectable by XRD, but which in total give rise to errors in chemical analyses (e.g., Ohr *et al.*, 1991). Such separates generally also contain illite or mica of more than one generation (detrital *vs.* authigenic) and composition; therefore, analyses may not be representative only of authigenic illite based on K/Ar data from shales (Pevear, personal communication, 1991).

Jiang *et al.* (1992) collated AEM analyses of illite and I/S as obtained from homogeneous material shown by TEM to be uncontaminated by other minerals or of 2:1 phases of more than one origin. With the exception of analyses of ammonium illite, the alkali totals are not significantly low, although there are apparent small alkali deficiencies relative to net negative charges as for the I/S analyses in Table 2, presumably because of alkali diffusion during analysis. Low alkali totals in AEM analyses may be caused by electron beam-induced diffusion (van der Pluijm *et al.*, 1988). In addition, alkali deficiency may be attributable to NH_4^+ (Juster *et al.*, 1987), and limited amounts of H_2O and/or H_3O^+ may be present in apparently unoccupied interlayer sites of some illite.

The chemical analyses used by Loucks (1991) as the basis for his conclusions that there are significant H_2O and H_3O^+ contents in illite are suspect because they were based on bulk analyses of clay separates. While they are valuable in many respects, bulk analyses should not be utilized for evaluation of detailed solid solutions because of the probable multiphase nature of the separates. Although we cannot directly analyze all specimens used in Loucks' study, the data reported here negate Loucks' prime example of illite with apparent extensive solid solution of "pyrophyllite hydrate" $[(H_2O)Al_2Si_4O_{10}(OH)_2]$ and "hydronium muscovite" $[(H_3O)Al_2Si_3AlO_{10}(OH)_2]$. The other analytical data used by Loucks are equally suspect in terms of representing one-phase illite and certainly should not be used to indicate the extent of its permissible solid solutions until high-resolution data confirm that they were obtained on single phases.

The question of the metastability of illite

Jiang *et al.* (1990a) concluded that illite is a metastable phase. Its composition (and that of rectorite, or R1 I/S) plots, to a first approximation, within the pyrophyllite–muscovite (or phengite) miscibility gap, which was inferred to show little mutual solid solution (Lippmann, 1981, 1982). In contrast, Loucks (1991) concluded that illite equilibrated with kaolin, quartz and water would contain solid solution of 50%–80% "hydronium muscovite" and 15%–35% "pyrophyllite hydrate." Together these substitutions would lead to a deficiency of around 80%–90% K^+ in the interlayer sites, such that EMPA data for illite should closely resemble those of pyrophyllite (as do some but not all of the EMPA data of Merino and Ransom, 1982). In contrast, AEM data for diagenetic Kettleman North Dome muscovite intimately associated with kaolin and quartz indicate few if any K^+ vacancies; therefore, this muscovite does not have more than a few percent of these occult components. Even the AEM analyses of I/S (Table 2) have K^+ contents of 1.3 per 12 [IV] + [VI] contents, far greater than that postulated by Loucks for illite equilibrated with kaolinite. Any small amounts of excess H_2O and H_3O^+ in interlayer sites of illite and other small deviations from the muscovite–pyrophyllite binary are unlikely to affect the phase relations (Jiang *et al.*, 1990a). Loucks' inferences of substitutions in illite and his phase diagrams are not supported by direct analyses of sheet silicates from the Kettleman North Dome. Loucks (1991) questioned the conclusions of Jiang *et al.* (1990a) regarding the metastability of illite based on inadequate analytical data. We, therefore, conclude that Loucks' inferences are unsubstantiated and that our previous conclusions regarding the metastability of illite have not been negated.

The H_3O^+ content of illite

Substitution of hydronium ion has not yet been adequately documented in silicates. While rare occurrences of hydronium jarosite are known (Alpers and Nordstrom, 1988), this phase forms in the anomalously low pH environment of acid sulfate ore deposits. Formation of hydronium may be favored under such conditions by progress of the reaction $H_2O + H^+ = H_3O^+$ to the right. However, micas are generally unstable relative to kaolinite, pyrophyllite, and alunite group minerals in such deposits (Jannas *et al.*, 1990; Li *et al.*,

1992). The widespread association of carbonates and iron oxides with illite in sedimentary basins is a contraindication of the highly acidic conditions required for the formation of hydronium ion and its substitution in phyllosilicates. Extensive hydronium substitution is, therefore, incompatible with the fluids associated with illite in ordinary sedimentary rocks. The authors conclude that significant solid solution of hydronium should not be expected in ordinary diagenetic illites.

ACKNOWLEDGMENTS

Special thanks are due to E. Merino for providing samples and associated information and to F. Lippmann for helpful suggestions and discussions. The authors are grateful for the reviews of M. Natthall and an anonymous reader. This work was supported by NSF grants EAR-88-17080 and EAR-91-04565 to D.R.P. The scanning electron microscope, scanning transmission electron microscope, and electron microprobe used in this work were acquired under NSF grants BSR-83-14092, EAR-87-08276, and EAR-91-04565, respectively.

REFERENCES

Ahn, J. H. and Peacor, D. R. (1986) Transmission electron microscopic data for rectorite: Implications for the origin and structure of "fundamental particles": *Clays & Clay Minerals* **34,** 180–186.

Alpers, C. N. and Nordstrom, D. K. (1988) Solid solution properties and deuterium fractionation factors for hydronium-bearing jarosites from acid mine waters: *Eos* **69,** 1480.

Burley, S. D. (1984) Patterns of diagenesis in the Sherwood Sandstone Group (Triassic), United Kingdom: *Clay Miner.* **19,** 403–440.

Essene, E. J. (1989) The current status of thermobarometry in metamorphic rocks: in *Evolution of Metamorphic Belts, Geol. Soc. Spec. Pub. 43,* J. S. Daly, R. A. Cliff, and B. W. D. Yardley, eds., Geol. Soc., London, 1–44.

Ireland, B. J., Curtis, C. D., and Whiteman, J. A. (1983) Compositional variation within some glauconites and illites and implications for their stability and origins: *Sediment.* **30,** 769–786.

Jahren, J. S. and Aagaard, P. (1992) Diagenetic illite-chlorite assemblages in arenites. I. Chemical evolution: *Clays & Clay Minerals* **40,** 540–546.

Jannas, R. R., Beane, R. E., Ahler, B. A., and Brosnahan, D. R. (1990) Gold and copper mineralization at the El Indio deposit, Chile: *J. Geochem. Explor.* **36,** 233–266.

Jiang, W.-T., Nieto Garcia, F., and Peacor, D. R. (1992) Composition of diagenetic illite as defined by analytical electron microscope analyses: Implications for smectite-illite-muscovite transitions: *Abstracts, 29th International Geological Congress, Kyoto 1992* **1,** p. 100.

Jiang, W.-T., Essene, E. J., and Peacor, D. R. (1990a) Transmission electron microscopic study of coexisting pyrophyllite and muscovite: Direct evidence for the metastability of illite: *Clays & Clay Minerals* **38,** 225–240.

Jiang, W.-T., Peacor, D. R., Merriman, R. J., and Roberts, B. (1990b) Transmission and analytical electron microscopic study of mixed-layer illite-smectite formed as an apparent replacement product of diagenetic illite: *Clays & Clay Minerals* **38,** 449–468.

Juster, T. C., Brown, P. E., and Bailey, S. W. (1987) NH_4-bearing illite in very low grade metamorphic rocks associated with coal, northeastern Pennsylvania: *Amer. Mineral.* **72,** 555–565.

Lanson, B. and Champion, D. (1991) The I/S-to-illite reaction in the late stage diagenesis: *Amer. J. Sci.* **291,** 473–506.

Li, G., Peacor, D. R., Essene, E. J., Brosnahan, D. R., and Beane, R. E. (1992) Walthierite, $Ba_{0.5}\square_{0.5}Al_3(SO_4)_2(OH)_6$, and huangite, $Ca_{0.5}\square_{0.5}Al_3(SO_4)_2(OH)_6$, two new minerals of the alunite group from the Coquimbo region, Chile: *Amer. Mineral.* **77,** 1275–1284.

Li, G., Peacor, D. R., Merriman, R. J., Roberts, B., and van der Pluijm, B. A. (1994) TEM and AEM constraints on the origin and significance of chlorite-mica stacks in slates: An example from Central Wales, U.K.: *J. Struct. Geol.* (in press).

Lippmann, F. (1981) Stability diagrams involving clay minerals: in *8th Conference Clay Mineral Petrology, Teplice 1979,* J. Konta, ed., Univ. Karlova, Praha, Czechoslovakia, 153–171.

Lippmann, F. (1982) The thermodynamic status of clay minerals: in *Proceedings of the 7th International Clay Conference, Bologna, Pavia, 1981,* H. van Olphen and F. Veniale, eds., Elsevier, New York, 475–485.

Loucks, R. R. (1991) The bound interlayer H_2O content of potassic white micas: muscovite–hydromuscovite–hydropyrophyllite solutions: *Amer. Mineral.* **76,** 1563–1579.

Macchi, L., Curtis, C. D., Levison, A., Woodward, K., and Hughes, C. R. (1990) Chemistry, morphology, and distribution of illites from Morecambe gas field, Irish Sea, offshore United Kingdom: *Bull. AAPG* **74,** 296–308.

Merino, E. (1975a) Diagenesis in Tertiary sandstones from Kettleman North Dome, California. I. Diagenetic mineralogy: *J. Sed. Pet.* **45,** 320–336.

Merino, E. (1975b) Diagenesis in Tertiary sandstones from Kettleman North Dome, California. II. Interstitial solutions: Distribution of aqueous species at 100°C and chemical relation to the diagenetic mineralogy: *Geochim. Cosmochim. Acta* **39,** 1629–1645.

Merino, E. and Ransom, B. (1982) Free energies of formation of illite solid solutions and their compositional dependence: *Clays & Clay Minerals* **30,** 29–39.

Morad, S. (1990) Mica alteration reactions in Jurassic reservoir sandstones from the Haltenbanken area, offshore Norway: *Clays & Clay Minerals* **38,** 584–590.

Norris, R. M. and Webb, R. W. (1990) *Geology of California:* 2nd ed., John Wiley & Sons, New York, 541 pp.

Ohr, M., Halliday, A. N., and Peacor, D. R. (1991) Sr and Nd isotopic evidence for punctuated clay diagenesis, Texas Gulf Coast: *Earth Planet. Sci. Lett.* **105,** 110–126.

Peacor, D. R. (1992) Diagenesis and low-grade metamorphism of shales and slates: in *Reviews in Mineralogy* **27,** P. R. Buseck and P. H. Ribbe, eds., Miner. Soc. Amer., Chelsea, 335–380.

Primmer, T. J. and Shaw, H. F. (1987) Diagenesis in shales: Evidence from backscattered electron microscopy and electron microprobe analyses: *Proceedings of the 8th International Clay Conference, Denver, 1985,* L. G. Schultz, H. van Olphen, and F. A. Mumpton, eds., The Clay Minerals Society, Bloomington, 135–143.

Pye, K. and Krinsley, D. H. (1983) Inter-layered clay stacks in Jurassic shales: *Nature* **304,** 618–620.

Reed, S. J. B. (1975) *Electron Microprobe Analysis:* Cambridge University Press, Cambridge, 400 pp.

Van der Pluijm, B. A., Lee, J. H., and Peacor, D. R. (1988) Analytical electron microscopy and the problem of potassium diffusion: *Clays & Clay Minerals* **36,** 498–504.

Van der Pluijm, B. A. and Kaars-Sijpesteijn, C. H. (1984) Chlorite-mica aggregates: Morphology, orientation, devel-

opment and bearing on cleavage formation in very-low-grade- rocks: *J. Struct. Geol.* **6,** 399–407.

Veblen, D. R., Guthrie, G. D., Jr., Livi, K. J. T., and Reynolds, R. C., Jr. (1990) High-resolution transmission electron microscopy and electron diffraction of mixed-layer illite/smectite: Experimental results: *Clays & Clay Minerals* **38,** 1–13.

Warren, E. A. and Ransom, B. (1992) The influence of analytical error upon the interpretation of chemical variations in clay minerals: *Clay Miner.* **27,** 193–209.

Weaver, C. E. and Pollard, L. D. (1973) *The Chemistry of Clay Minerals:* Elsevier, New York, 213 pp.

(Received 20 October 1992; accepted 1 September 1993; Ms. 2288)